# Thermal performance evaluation of a passive building wall with $CO_2$-filled transparent thermal insulation and paraffin-based PCM

Agustín Torres-Rodríguez[a], David Morillón-Gálvez[b], Daniel Aldama-Ávalos[c], Víctor Hugo Hernández-Gómez[d], Ivan García Kerdan[b,e,f,*]

[a] Facultad de Arquitectura, Universidad Nacional Autónoma de México, 04510, CDMX, México
[b] Instituto de Ingeniería, Universidad Nacional Autónoma de México, 04510, CDMX, México
[c] Facultad de Estudios Superiores Aragón, Universidad Nacional Autónoma de México, 57178 Estado de México, México
[d] Facultad de Estudios Superiores Cuautitlán, Universidad Nacional Autónoma de México, 54716, Estado de México, México
[e] Department of Built Environment, School of Design, University of Greenwich, Old Royal Naval College, Park Row, London, SE10 9LS, UK
[f] Department of Chemical Engineering, Imperial College London, South Kensington Campus, London, SW7 2AZ, UK

## Abstract

Novel thermal insulation materials and wall configurations have the potential to play a major role in reducing energy demand and carbon emissions from the building sector. In this study, a passive heating wall system composed by a $CO_2$-filled transparent thermal insulation (TTI) and an organic phase change material (PCM), and a passive cooling system composed by a Tromble Wall with nano-film and a $CO_2$-filled TTI are proposed and evaluated. The aim is to present a detailed analytical model for rapidly calculating thermal performance of the proposed wall configurations. As case study, a 108 $m^2$ south façade of a building located in Mexico has been used. Outputs suggest that as a passive heating measure, the system has the potential to supply heat in the order of 118 W, 126 W, 134 W, and 157 W, during the months of December, January, February, and March respectively. Additionally, thermal performance and air velocity simulations suggest that for the heating case, considering an outdoor and indoor temperature conditions of 0 °C and 21 °C respectively, the internal layer surface reaches a temperature of 9.2°C; while for the cooling case, considering outdoor and indoor temperature conditions of 25 °C and 21 °C respectively, it reaches 22.5 °C with a maximum indoor air velocity of 0.5 m/s. Compared to other gases, $CO_2$ could hold a greater potential due to its low thermal conductivity and capital costs. Large-scale implementation of such systems could make the building sector an interesting option as an artificial sink for carbon storage.

**Keywords:** building envelope; organic phase change material; passive system; mathematical model; transparent thermal insulation.

## Nomenclature

| Symbol | Name | Unit |
|---|---|---|
| A | *Aspect ratio (length divided by hydraulic diameter)* | - |
| a | *Coefficient for calculating the g-value of the TTI system* | - |
| $A_{swh}$ | *Total area of solar wall heating* | $m^2$ |

* Instituto de Ingeniería, Universidad Nacional Autónoma de México, 04510, CDMX, México.
E-mail address: IGarciaK@iingen.unam.mx ; i.garcia-kerdan@imperial.ac.uk (I. García Kerdan).

| | | |
|---|---|---|
| $CP_{pcm}$ | *Specific heat of PCM* | kJ/kg K |
| $D_h$ | *hydraulic diameter* | Mm |
| $F_c$ | *Reduction factor due to shading devices* | - |
| $F_f$ | *Reduction factor due to the frame area* | - |
| $F_s$ | *Reduction factor due to natural shading* | - |
| g | *Total solar energy transmittance* | % |
| $g_{TTI,h}$ | *Total solar energy transmittance* ($g_{h,b}/\{1+[R_s/(R_{se}/(R_{se}+R_b)]\}$) | % |
| $g_{TTI,m,\ j}$ | *Transmittance with monthly orientation m* ($g_{TTI,M,\ j} = g_{TTI,h} - a_{M,j}\ g_{TTI,n}$) | % |
| $h_{con}$ | *Convective coefficient of air* ($h_{conv} = (k_{wall}\ Nu) / L$) | $W/m^2\ K$ |
| $I_s$ | *Solar irradiation* | $J/m^2$ |
| $Is_{,M,I}$ | *Month solar irradiation* | $W/m^2$ |
| $k_{Wall}$ | *Thermal conductivity of wall with nano-film* | $W/m^2\ K$ |
| L | *Distance between the beginning of the capillary tube filled with $CO_2$ gas, and the point at which the refracted ray hits the interior surface of the tube* | Mm |
| $L_{pcm}$ | *Latent heat of PCM* | Day/m |
| $M_{pcm}$ | *Mass of PCM* | J/kg |
| $m_s$ | *Sand mass* | Kg |
| Nu | *Nusselt number* ($Nu = h_{Conv}\ L / k_{wall}$) | - |
| n | *Average number of cell wall interactions for the incoming light beam* ($n = \frac{2Ltan(\theta_3)}{D_h}$) | - |
| $Q_{pcm}$ | *Heat available* ($Q_{pcm} = m_{pcm}\ CP_{pcm}\ \Delta T + m_{pcm}\ L_{pcm}$) | kJ |
| $Q_s$ | *Solar heat gain* | J |
| $Q_{swh,hp,South,Month}$ | *Heat gain during one month* | J |
| $Q_{TTI}$ | *Rate of heat flow of TTI* | W |
| $Q_{TW}$ | *Rate of heat flow of Trombe wall* | W |
| R | *Thermal resistance* | $m^2\ K/W$ |
| Ri | *Refraction index* | - |
| $S_{TTI}$ | *Surface of TTI* | $m^2$ |
| $S_{wall}$ | *Wall surface* | $m^2$ |
| $T_{avg.\ duct\ air}$ | *Average temperature of duct air* | °C |
| TC-TW | *Thermal Catalytic Trombe Wall* | - |
| $T_{inlet.\ duct\ air}$ | *Inlet temperature of duct air* ($(T_{outlet\ duct\ air} + T_{inlet\ duct\ air}) / 2$)) | °C |
| $T_{outlet.\ duct\ air}$ | *Outlet temperature of duct air* | °C |
| $T_1$ | *Temperature on nano-film* | °C |
| $T_2$ | *Absorber temperature* | °C |
| Z | *factor of correction by orientation* | - |

## Greek symbols

| Symbols | Name | Unit |
|---|---|---|
| $\alpha_s$ | *Absorptance of solar radiation* ($\alpha_s = 1 - \tau - \rho$) | % |
| $\varepsilon_{abs}$ | *Absorber emission* | % |
| $\rho_s$ | *Solar reflectance* | % |
| $\theta_1$ | *Angle of incidence in the first medium* | Degrees |

| | | |
|---|---|---|
| $\theta_2$ | *angle of refraction in the second medium* ($\theta_2 = sen^{-1}$ [$(ri_{air}\ sen\theta_1) / ri_{glass}$]) | *Degrees* |
| $\theta_3$ | *angle of refraction in the third medium* ($\theta_3 = sen^{-1}$ [$(ri_{glass}\ sen\theta_2) / ri_{CO2}$]) | *Degrees* |
| $\tau(\theta_3)$ | *transmittance of solar radiation in the third medium* | *%* |
| $\tau_s$ | *Solar transmittance* ($\tau=1-\alpha_s-\rho$) | *%* |

## Subscripts

| *Symbols* | *Name* |
|---|---|
| *b* | *hemispherical irradiation of TTI system* |
| *hp* | *Heating period* |
| *hpz* | *Heating period defined by factor Z* |
| *j* | *Orientation in month M* |
| *n* | *Normal irradiation* |
| *s* | *Air gap* |
| *se* | *Exterior surface* |
| *si* | *Interior surface* |
| *so* | *South* |
| *swh* | *Solar heating of wall with TTI system* |
| *TTI+PCM* | *TTI system plus organic PCM (PW)* |
| *W* | *Wall* |

## 1. Introduction

Olgyay (1963), one of the pioneers of solar building design, applied solar control, natural ventilation and shading design to several buildings in the United States, illustrating the importance of using passive systems in achieving thermal comfort. Similarly, Szokolay (2004), apart from the extensive studies in passive systems, such as night and cross ventilation, and evaporative cooling, illustrated how a massive wall exposed to solar radiation acted as a heat collector and storage device (also known as the Trombe-Mitchel system).

Yeang (2001) concluded that passive systems can increase the economic value of a building (between 5 and 10%) and depending on the geographical location and local energy prices, amortization periods could be around 5-15 years. In this sense, Parker and Brown (2013) proposed to incorporate passive systems as a strategy not only for reducing building energy consumption but also for reducing the operating costs, as these systems commonly require low-maintenance due to small amount of moving devices. These authors also affirmed that an optimum passive design can provide useful solar gains to uncomfortable space in the winter.

Trombe Wall (TW), a typical passive building system, composed by a thermal mass and a glazing system located between the outside environment and the indoor space, allows for solar radiation that hits the thermal mass to be captured as heat energy. This way, the TW acts as an energy storage device so that this stored energy can be used later to provide heating to the adjacent indoor spaces. Recently, Chel and Kaushik (2018) recommended a TW with transparent honeycomb panels as a method to reduce energy demand in buildings and affirmed that the design showed good potential

for winter heating. However, Szokolay (2004) suggested using Heating, Ventilation and Air Conditioning (HVAC) systems as complementary mechanical systems, where assembly of natural and architectural components cannot completely ensure thermal comfort.

Hernández et al. (2006) presented an analytical model to simulate the thermal behavior of solar heat discharge wall systems. An empirical study was conducted to compare the results from the proposed model with those from the laboratory. Later, Hernández et al. (2010) provided design recommendations to improve the performance of the systems. The authors modified design parameters to form a heat discharge system (e.g. air gap dimensions, system's height and width, air channel opening dimensions) aiming at reducing the risk of overheating. Finally, using similar principles for the walls, Hernández and Morillón (2013) proposed a model to calculate the thermal performance of double skin roofs. The authors proposed an analytical model that has been validated by the performance of an experimental prototype.

Kundakci Koyunbaba and Yilmaz (2012) simulated and compared two TW systems with single and double glazing in Izmir, Turkey. The authors found that double glazing systems had a higher insulation capacity during the night period than single glazing, but the latter supplied higher heat gains to the room during daytime due to higher heat transfer. Thus, the authors suggested using single glazing with a shutter for night-time to avoid heat losses during the winter period. They also recommended improving these passive systems for summer cooling to prevent overheating. Briga Sá et al. (2017) analyzed the temperature fluctuations on the air gap of an experimental TW by considering the effect of ventilation openings and shading devices. The device was designed, constructed, instrumented and monitored in Vila Real, Portugal. By opening and closing the air vents between 2-3 hours after the sunrise and one hour before the sunset, the authors observed higher temperatures at the top of the air layer compared to the base. When the ventilation openings were closed, and the shading mechanism was not operated, the temperatures at the top were around 19 °C higher than those monitored at the bottom.

Veinberg and Veinberg (1959) cited by Kaushika and Sumathy (2003) examined the use of deep narrow meshes such as solar transparent honeycomb covering and Transparent Thermal Insulation (TTI) comprised of capillary tubes made of glass or plastic. Huenchuñir (2002) suggested a physical description of a TTI system, where the perimeter must be hermetically sealed, and the gaps are recommended to be filled with an inert gas such as argon or krypton. The dimensions of hermetically sealed panels should be limited to a minimum of 1,000 x 1,000 mm and a maximum of 2,000 x 2,000 mm. For widths and heights of more than 1,300 mm, the capillary slab needs to be divided into T-profiles. In this case, the capillary slab needs to be assembled in two or more pieces. In terms of materials, plastics including polycarbonate and acrylic were suggested. As a result, the glass used for the TTI can be found with an exterior diameter of 7 or 10 mm and can reach temperatures up to 265 °C. According to Huenchuñir (2002) the benefits of the TTI system as a part of a passive building design can be summarized as follows:

1. Depending on the TTI system, the rate of heat flow can reach between 100 kW/m$^2$ to 200 kW/m$^2$ during the winter season.
2. Paints on the absorber can reach an absorption rate of 90%.
3. TTI system that uses glass tubes with a 7 mm outer diameter and a length of 80 mm can reach a temperature of 265 °C.

4. TTI systems with polycarbonate cells can reach a temperature of 140 °C.

Platzer (1997) analyzed a TTI system that was comprised of glass tubes with diameters of 7 to 9 mm, filled with air and an exterior wall with thickness of around 100 μm. The author found that the transmittance (dimensionless number) for direct solar radiation was 0.82 and for diffuse solar radiation was 0.67. Kaushika and Arulanantham (1995) developed an analytical model to evaluate the refraction, reflection, and absorption into transparent honeycomb insulation material. It was reported that this TTI system had an exterior wall with a thickness of 5 cm and emissivity factor of 0.85.

Hauser et al. (1996) evaluated energy performance of six commercial TTI systems in Austria. The researchers concluded that depending on the system and the climate location, it was possible to achieve a heat transfer of around 100 to 180 kWh/$m^2$-year in the city of Vienna and around 450 kWh/$m^2$-year in houses with south-facing orientation located in high mountain regions of Austria. Platzer (1999) proposed a steady-state mathematical model to simulate thermal behavior of the heating system with two wall insulation types (T and O). The model included parameters such as solar energy absorption, solar reflection, total energy transmittance of the TTI system, system´s thermal resistance with an integrated absorber, air gap, reduction factor due to shading and sun protection, and average solar radiation.

Athienitis and Ramadan (2000) developed an experimental prototype of a TTI system consisting of an exterior single glazing protector, an air cavity, a Lexan transparent honeycomb, a second air cavity, thermal storage with concrete wall, a third air cavity, and an interior gypsum board layer, with south-facing orientation. The experimental prototype, tested in Montreal, Canada, reached a heating capacity of 550 W/$m^2$ on a clear-sky day. Also, it was found that the air temperature in the building room with the TTI system was lower than 30 °C on a cloudy cold day, and 20 °C on a sunny day. The researchers concluded that a roller blind control should be integrated on the system to exclude unwanted solar gains. Ochs et al. (2000) designed a method to calculate heat flow rate of a passive wall with TTI. The wall's thermal resistance was 0.10 $m^2$ W/°C with a depth of 25 mm for air gap, and an emissivity of 0.90. The TTI, tested in Switzerland, reached a temperature of 80 °C on a surface without an integrated absorber during the winter season. Wallner et al. (2006) developed a TTI system made of cellulose triacetate polymer film that was used on a south-facing wall of house in Graz, Austria during August. The maximum weekly average room temperature was found to be at 28 °C and the maximum temperature of absorber was about 75 °C. Heat gain fluxes were higher than 50 W/$m^2$.

Additionally, Phase Change Materials (PCM) have been widely investigated as building insulation materials in different configuration types. Reim et al. (2005) measured and computed thermal conductivity of a TTI system filled with silica aerogel granules and gases such as $CO_2$ (14.5 x$10^{-3}$ W/m K), air (15.3 x $10^{-3}$ W/m K), argon (15.0 x $10^{-3}$ W/m K) and krypton (13.5 x $10^{-3}$ W/m K) at a pressure of 1,000 Pa. Cuce et al. (2014) concluded that aerogel-filled TTI can also be used for solar control and passive heating on the external walls of buildings. The material has a high transmittance, although it loses its physical structure and transparency in contact with water. Buratti and Moretti (2011) compared a window with monolithic aerogel, a window with air in the interspace and a low-e layer. The window with aerogel had a thermal conductivity of 0.010 W/mK and was able to reduce heat losses by 25% with respect to the window filled with air.

According to Lokesh et al. (2009), a PCM in its solid phase and with thickness of 4 mm can be a suitable transparent insulating material if it has a thermal conductivity of 0.34 W/m K, a latent heat of fusion of 236.17 kJ/kg°C and a transmittance of 0.676 to an ambient temperature of 38.7 °C. Thirugnanam and Marimuthu (2013) analyzed the behavior of latent heat of Paraffin Wax (PW) and recommended a melting temperature of around 40-60 °C for selecting PCM in the heating and cooling applications for buildings. Difficulties, as flammability and high-volume changes between solid and liquid stages of PW, can be resolved with a proper design of the container. Mohd et al. (2010) combined copper foam with microencapsulated PW to heat up the interior air of a house in Malaysia. The PW has a melting and solidification temperature of 26.1 °C and a suggested melting temperature of 1 to 3°C above the average temperature room to achieve the optimal diurnal heat storage; while the copper foam, with a thermal conductivity of 350 W/m K, act as a heat transfer medium towards the interior air of a room. Mohd et al. (2010) also suggested paraffin as it could store up to 330 W/m$^2$ K. Considering a total area of 8.56 m$^2$ used in the building façade, the baseline cooling load of 1.46 kWh dropped 0 kWh. The drop-in cooling load due to the integration of PW into the building façade was achieved as this construction method could store the heat during the daytime and discharge it back to outside at night.

Ji et al. (2009) studied the thermal behavior of a TW in a building located in Xining, China. The TW had an exterior wall covered with 0.5 mm steel panel and 100 mm polystyrene aiming at increasing the temperature of the air duct. The results show that heat gains increased from 11,139.4 kJ in the conventional TW system to 17,387.6 kJ in the improved TW system improving operating efficiency by 56 % in comparison with conventional TW system (21.69 %). Konstantinidou (2010) used EnergyPlus to simulate a system comprised of two glass sheets and macro-encapsulated PW with thickness of 3 mm of an interior layer of the exterior south façade, located at the University of Texas in Austin. Based on the simulated outputs, the authors suggested that the surface area of the PCM should be maximized, while the material thickness did not show any considerable effect in the increase and/or decrease of the building's cooling peak load.

The thermal conductivity of PCM is another parameter that has been studied extensively (Berge and Johansson, 2012). Lokesh and Sharma (2009) showed that the transmittance of the solar radiation of the liquid phase PCM is higher than that of water, when PCM and water were used as a filling with the same thickness in a TTI system. Vadwala (2011) concluded that using open cell metal foam with high porosity (> 85%) can enhance the heat transfer of the PCM due to its high thermal conductivity and high surface area density. The author found that the thermal conductivity of a foam-wax composite was 3.8 W/mK, which was 18 times higher than 0.21 W/mK of purely PW.

Wong and Eames (2015) modelled solar transmittance, absorptance and reflectance of encapsulated KAPILUX Capillary System. Five angles (0°, 40°, 55°, 70° y 80°) of solar incidental rays were used on equations to calculate the optical properties of complex layers of TTI. This type of numerical modelling technique could benefit from considering the incidental angle of solar beam radiation. Bendong et al. (2018) proposed a thermal-catalytic-Trombe wall (TC-TW) system to insulate and to purify the air of a building located in Hefei, China. The study shows that compared to a conventional Trombe system; the TC-TW system has the potential to reduce the monthly total heating load by 28.3 %. The system was able to reduce up to 45 MJ/m2. To achieve

this thermal reduction, the authors had to add an insulation layer with thermal conductivity of 0.035 W/mK and thickness of 20 mm between the catalytic layer and the wall.

Paneri et al. (2019) described a modular set of TTI system and PCM (GLASSX AG-products). This architectural application considered a cavity filled with inert gas and a cavity with PCM plate (Calcium chloride hexahydrate). These authors showed 131 commercial applications of TTI systems where the gas cavity sometimes was filled either with air, aerogel or krypton. Also, the study illustrated the development of nanoparticle-polymer composite film which was integrated into a multi-pane window system as a thermal insulation. The authors detailed the type of TTI facades able to reduce thermal losses and energy consumption. Swirska-Perkoswka et al. (2020) analyzed a building envelope covered with a TTI system located in Poland, using a finite-difference method and thermal conduction equations in the heating period. Compared to the south facing wall, the study found that the annual heat gains on western and eastern facing walls decreased by 24-31%. The authors suggest an optimal thickness between 88 and 108 mm the for the TTI system for the studied climate.

To the best of the authors' knowledge there is still a lack of studies that investigate the heat transfer performance of wall configurations, considering the integration of transparent thermal insulation (TTI) systems and phase change materials (PCM). Thus, the aim of this study is to develop an analytical model to calculate the rate of the heat flow of the proposed wall configuration and compare the obtained outputs with those from the complex simulation models typically used in commercially available tools. To test the model, the proposed TTI has been filled with carbon dioxide ($CO_2$) due to lower thermal conductivity compared to air and argon at a pressure of 1,000 Pa. The rate of heat flow is computed to compare it with the rates of other gases such as air, argon and krypton. Moreover, a control system of the heat flow for heating and cooling passive system has been used to avoid overheating of the room air in the summer season.

This study is organized as follows. First, the wall configuration and calculation methods are presented. Next, typical simulation of the wall’s configuration is presented. Following, the study shows the obtained results from the proposed mathematical model. Finally, conclusions and suggestions for future work are presented.

## 2. Materials and methods

### *2.1 Passive Wall Components*

#### *2.1.1 Passive Heating System*

A new passive heating system wall configuration is proposed in this study. The proposed wall configuration considers a TTI with an integrated absorber comprised of the following five components: i) glass cover, ii) honeycomb board, iii) absorber, iv) exterior wall, and v) paraffin panel. In such system, the heat due to solar radiation would flow through a glass cover toward the honeycomb board. Then, the heat would flow towards the absorber, where it would be transferred by conduction through the wall/paraffin board and by convection through the interior air of the

room. Fig, 1 summarizes the proposed heating system, illustrating the TTI components, the thermal resistances, and *g* value of the system (0.44).

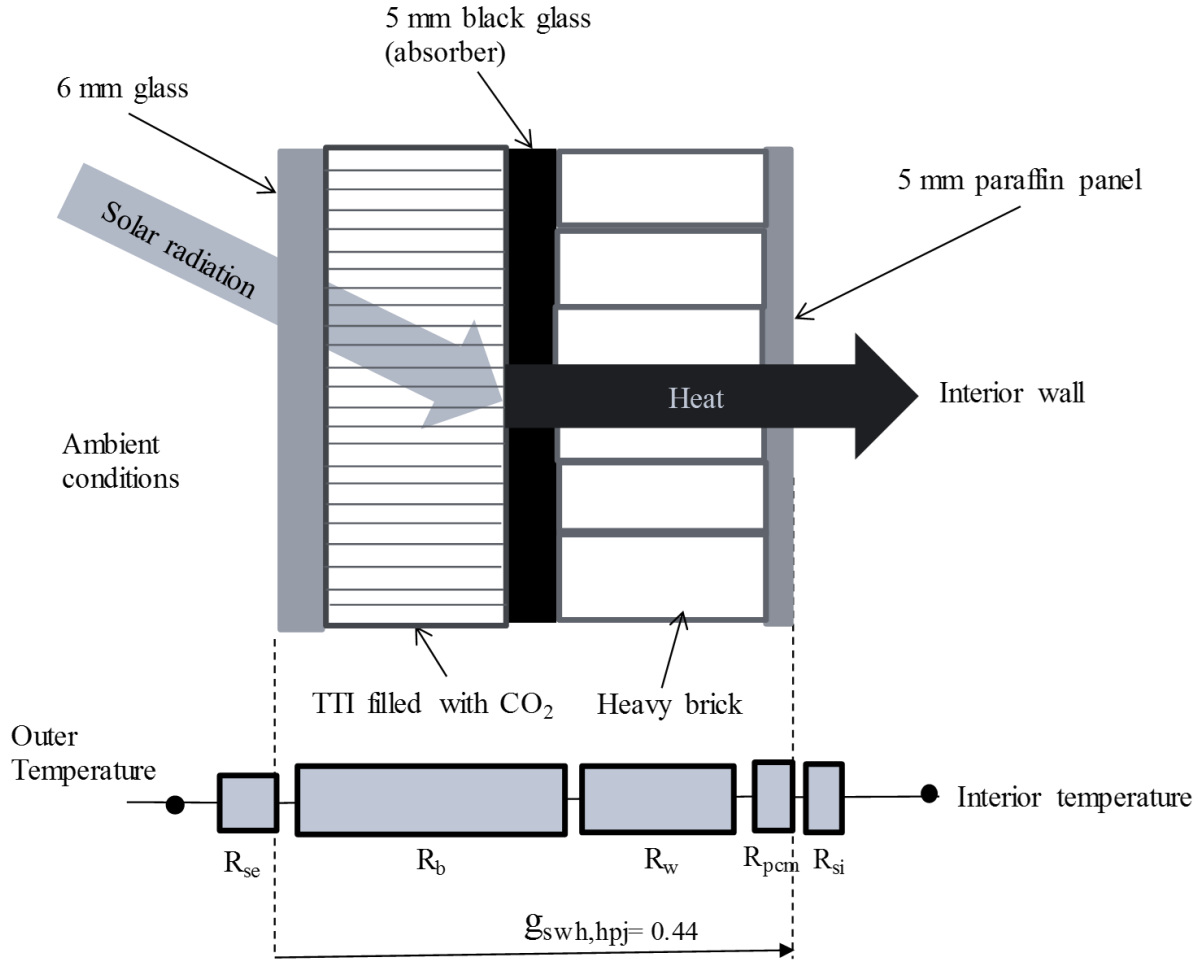


**Fig. 1. Diagram of the proposed wall configuration as well as resulting thermal resistances and g-value.**

In this study, the following physical characteristics are considered:

- The interior wall is an opaque device and has integrated an absorber where the brick is located between the glass plate and the paraffin.

- There is no air gap between the TTI element and the interior wall.

- The boundary between the TTI and the interior wall is the outside surface of the wall. Circular capillary slabs with a length of 20 mm, diameter of 5 mm and filled with $CO_2$ can be found. $CO_2$ has been proposed for use within the TTI due to low thermal conductivity (0.0145 W/m K). Cuce and Riffat (2015) indicated that this value is below 0.020 W/mK.

- The PCM is a mixture of ethylene-based polymer (40%) and PW (60%) laminated on both sides with a 100 μm-thick aluminum sheet. DuPont (2011) states a value of thermal

conductivity for paraffin, in solid phase, of 0.18 W/mK, a melting point of 21.7 °C and solidification of 18 °C.

### *2.1.2 Passive Cooling System*

For the cooling case, cold air would be supplied through a low opening in the wall. This way, the heated air, supplied by the TTI system, will be sent toward the top of the wall while the black foil would absorb the heat from solar radiation, sending it toward the air gap. Part of this heat will be rejected by the TTI system and the remainder will be reflected.

The architectural elements of the passive cooling system, illustrated in Fig. 2, includes the following:

- Glass plate, thickness of 5 mm.
- The TTI is filled with $CO_2$ gas and the lengths of the capillary tubes are 100 mm.
- The absorber panel is black in color and 1 mm wide. This black foil is made of copper.
- Nano-film has a thickness of 8 µm thick and is applied to the wall.
- The brick has a thickness of 100 mm.
- The space between the absorber panel and nano-film is 150 mm. The nano-film is made from metallic oxide that is highly reflective of thermal radiation. It is located on the wall to avoid the heat flow by convection through it. In the cooling period, it would absorb solar radiation and will use it to heat the glass. This creates a thermal barrier which diminishes solar heat gain (Wasser Resources, 2020).
- The top wall opening is 25 cm and is under roof of concrete.
- The lower wall opening is 15 cm on floor of marble slab.

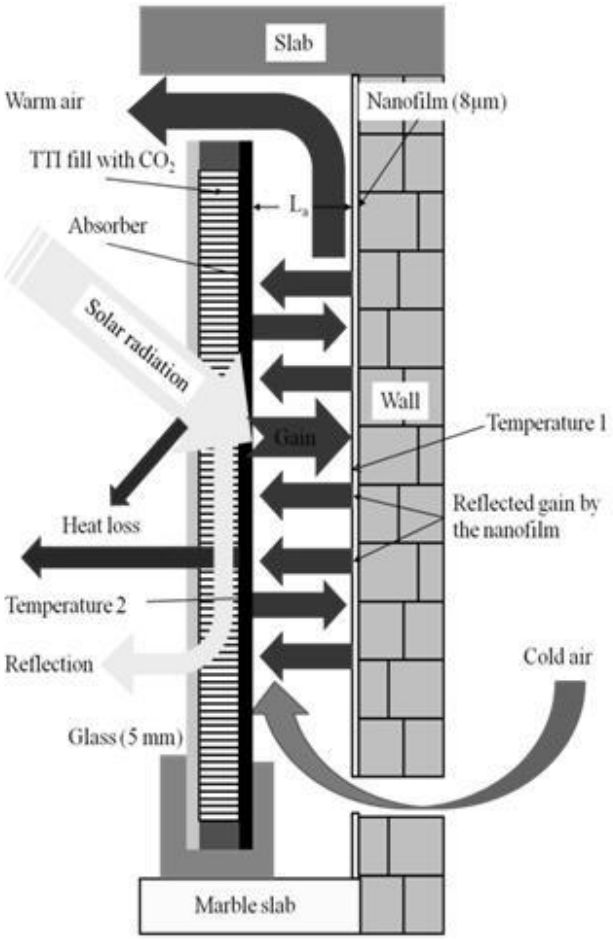


**Fig. 2. Devices of passive cooling system.**

The considered nano-film applied to the wall is a shield against the heat flow that comes from a black absorber. Marble slab supplies diffuse radiation toward the absorber and the air gap. In this system, copper is considered to have a thermal conductivity of 373.2 W/mK (SENER/CONUEE, 2001) and can be used as a black absorber material.

### *2.2 Proposed analytical model*

#### *2.2.1 Procedure for calculating the heat flow rate of TTI and PW*

In this section, a novel analytical model is proposed. The following procedure has been followed:

(1) First, the basic characteristic values of the TTI element must be known such as a total solar energy transmittance in heating mode and irradiation hemispherical in the element of the TTI ($gh_b$), a total solar energy transmittance and normal irradiation in the element of the TTI ($g_{nb}$), and a thermal resistance of the TTI element to hemispherical irradiation ($R_b$).

(2) For the case of the TTI element without an integrated absorber and if the solar absorptance $\alpha_s$ of the wall surface is smaller than 0.90, the solar radiation transmittance $\tau_{hb}$ and $\tau_{nb}$, and

the reflectance $\rho_{hb}$ of the TTI element should be known ($\rho_{hb}$ may be assumed to value of 0).

(3) The thermal resistance $R_W$ of the brick wall must be of 0.159 $m^2$ K/W (Pérez et al., 2011) for a brick layer.

(4) Based on Dupont (2011), a thermal conductivity of 0.18 W/m K for PCM in a solid state and 0.14 W/mK in a liquid state for organic PCM ($k_{pcm}$) has been considered.

(5) The thermal resistance of ambient air was assumed to be 0.08 $m^2$ K/W ($R_{se}$) and and of the interior room air of 0.12 $m^2$ K /W ($R_{si}$).

(6) The total solar energy transmittance ($g_{TTI,h}$), the transmittance with monthly orientation m ($g_{TTI,m,j}$), and the transmittance on the solar wall during the heating period ($g_{swh,hp,j}$), are computed by using equation (1), $g_{TTI,h}$ and $g_{TTI,m,j}$ . The equations have been suggested by Platzer (1999).

$$g_{swh,hp,j}=g_{TTI,hp,j}=(R_{se}+R_b+R_s) / (R_{se}+R_b+R_s+R_w+R_{pcm}+R_{si}) \quad (1)$$

Equation (1) was modified with the thermal resistance of the PCM and the factor coefficient $z_j$ which is showed in Table 1.

**Table 1. Factors $Z_j$ depend on orientation (Platzer, 1999).**

| Orientation j | S | SW/SE | W/E | NW/NE | N |
|---|---|---|---|---|---|
| Z | 1.04 | 1.02 | 0.98 | 0.99 | 1.00 |

The monthly heat flow rate of the TTI-PCM can be calculated as follows (Platzer, 1999):

$$Q_{swh,hp,j} = A_{swh,j} F_f F_s I_{s,M,j} g_{swh,hp,j} \quad (2)$$

While for winter season, Platzer (1999) made the following approximation:

$$g_{TTI,hp,Zj} = g_{TTI,h,Zj} \quad (3)$$

The g-values $g_{TTI,hp,j}$ and $g_{swh,hp,j}$ of the TTI system and the solar heat gain $Q_{swh,hp,j}$ need to be obtained. During the heating period, Platzer (1999) recommended computing the constant g-values with the following equation:

$$g_{TTI,hp,j} = g_{TTI,h} - a_{hp,j} g_{TTI,n} \quad (4)$$

A more precise approximation is also given by Platzer (1999) with the following equation:

$$a_{hp,j}=\Sigma M a_{m,j} I_{s,m,j} / \Sigma M I_{s,m,j} \quad (5)$$

The following equation was suggested by Thirugnanam and Marimuthu (2013) in order to compute the heat available ($Q_{pcm}$) of PW.

$$Q_{pcm}=m_{pcm}CP_{pcm}\,\Delta T + m_{pcm}\,L_{pcm} \quad (6)$$

### *2.2.2 Theoretical analysis of the optical properties of the TTI as a passive system*

Furthermore, theoretical analysis can be used to determine the optical properties and the rate of heat flow of the TTI system, made of different materials for a circular honeycomb cell. The optical properties of the TTI materials were defined by Cengel (2004). According to Wong et al. (2007), the summation of all individual rays transmitted through the circular honeycomb cells at the TTI can be determined by using the following equation:

$$\tau(\theta) = [\tau_s + \rho_s]^n = [1-\alpha_s]^n \quad (7)$$

Where $\tau(\theta)$ is the transmittance of the solar radiation in a medium with an incidental angle $\theta$, $\tau_s$ is the solar transmittance, and $\rho_s$ is the solar reflectance. Wong et al. (2007) also suggested that for a circular honeycomb cell, n = 2A tan ($\theta$). Fig. 3 shows an array of a circular honeycomb cell with an incident, reflected, and refracted rays over a glass filled with $CO_2$.

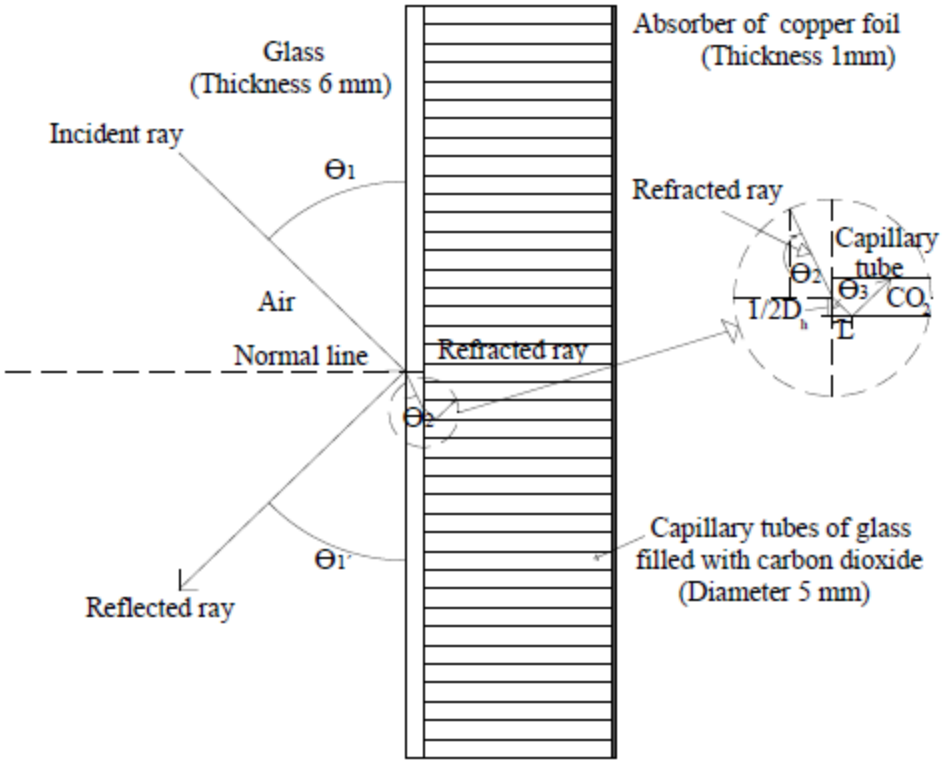


**Fig. 3. Array of circular honeycomb cells with incident ray and reflected ray.**

### *2.2.3 Derivation of the mathematical model*

To compute the rate of heat flow of a passive system (TTI-wall with nano-film), a new mathematical model has been developed as follows.

According to Snell´s law and Fig. 3,

$$ri_{air}\ sen\theta_1 = ri_{glass}\ sen\theta_2 \quad (8)$$

and

$$ri_{glass}\ sen\theta_2 = ri_{CO2}\ sen\theta_3 \quad (9)$$

thus, $\theta_2$ y $\theta_3$ can be computed.

The calculation of ratio (A) was suggested by Wong et al. (2007) as follows

$$A = L / D_h \quad (10)$$

and

$$\tan(\theta_3) = [D_h / 2L] \quad (11)$$

then

$$2\tan(\theta_3) = [D_h / L] \quad (12)$$

and

$$2\tan(\theta_3) = 1 / A \quad (13)$$

clearing A of Eq. (12)

$$2A\tan(\theta_3) = 1 \quad (14)$$

Equation (14) shows $2A\tan(\theta_3) = 1$. Then, solar transmittance in Eq. (7) is computed to

$$\tau(\theta) = [2A\tan(\theta_3) - \alpha_s]^n \quad (15)$$

with $A = L/D_H$, it yields

$$\tau(\theta_3) = [2L\tan(\theta_3) / D_h) - \alpha_s]^n \quad (16)$$

As the heat flow rate in the TTI system is affected by the solar transmittance $\tau(\theta_3)$ in capillary tubes of glass filled with $CO_2$, this rate is calculated as follows

$$Q_{TTI} = S_{TTI}\varepsilon_{abs}\sigma\tau(\theta_3)(T_{avg}^4 - T_2^4) \quad (17)$$

Heat transfer by conduction and convection between two components of the passive heating system can be calculated with the following equation

$$Q_{TTI} = Q_{TW} \quad (18)$$

The rate of heat flow that enters inside of the room can be calculated as follows:

$$Q_{TW} = h_{cov}s_{wall}[(T_1 - T_{avg.\ duct\ air})] \quad (19)$$

as

$$h_{conv} = (k_{wall}\,Nu) / L \quad (20)$$

where *Nu* is Nusselt number and *L* is the Distance between the beginning of the capillary tube filled with CO2 gas, and the point at which the refracted ray hits the interior surface of the tube. Thus, if $h_{conv}$ is substituted into equation (19), it yields:

$$Q_{TW} = [k_{wall}NuS_{wall}(T_1 - T_{avg.\ air\ duct})] / L \quad (21)$$

Cengel (2004) suggested computing the temperatures $T_1$ and $T_2$ of a TW using the finite element method.

## 3. Simulations

### *3.1 TTI system with integrated absorber*

Before applying the developed analytical model, a computational simulation of the TTI system for a building located in Mexico City has been performed. At daytime, the TTI system receives the heat from solar radiation, flowing through the wall and PCM until it reaches the interior room air. At night, the PCM will receive the heat from internal sources such as equipment, lights and people, transferring it through the wall, the TTI system and finally being released to the ambient. The main characteristics of the TTI elements are assumed as follows:

- The $R_{se}$ is assumed at 0.08 $m^2$ K/ W.
- As suggested by Cuce and Riffat (2015), glass with a thickness of 6 mm has a thermal conductivity of $\lambda$ = 0.18 W/m K.
- As suggested by Reim et al. (2005), thermal conductivity of $CO_2$ gas, contained in capillary tubes, yields a thermal resistance of 0.18 $m^2$ K/W. The total thermal resistance of the TTI element to hemispherical irradiation (**$R_b$**) has been assumed at 3.12 $m^2$ K/W
- The massive wall is made of heavy bricks with thickness of 12 cm and a thermal conductivity of $\lambda$ = 0.814 W/m K.

- The PW panel has a thickness of 5 mm and a thermal conductivity of $\lambda = 0.18$ W/m K.
- $R_{si}$ has been assumed as 0.123 $m^2$ K/W when the TTI system performs as a passive heating system at daytime.
- In January, the values of the total energy transmittance of an air gap in the heating period are modified with a factor ($Z_{so}$) and a coefficient ($a_{hp,s}$) as follows.

$$g_{TTI,hp,S} = g_{TTI,h} - a_{hp,s}\, Z_{so}\, g_{TTI,n} = 0.43 - (-0.075)(1.04)(0.62) = 0.48$$

Table 2 summarizes the parameters used in the simulation.

**Table 2 Summary of the parameters for passive heating system in the winter season.**

| **Parameter** | $g_{h,b}$ | $g_{n,b}$ | $R_b$ $m^2K/W$ | $R_{se}$ $m^2K/W$ | $\alpha_s$ (black copper foil) % | $A_{jan,south}$ | $A_{feb,south}$ | $A_{mar,south}$ | $A_{dec,south}$ | $\sum a_{month,south}$ | $I_{s,jan,south}$ $W/m^2$ |
|---|---|---|---|---|---|---|---|---|---|---|---|
| **Value** | 0.49 | 0.62 | 3.12 | 0.08 | 0.9 | -0.105 | -0.067 | -0.023 | -0.105 | -0.3 | $1.6x10^7$ |

| **Parameter** | $I_{s,Feb,South}$ $W/m^2$ | $I_{s,mar,south}$ $W/m^2$ | $I_{s,dec,south}$ $W/m^2$ | $\sum I_{s,month,south}$ $W/m^2$ | $a_{hp,january,south}$ | $a_{hp,feb,south}$ | $a_{hp,mar,south}$ | $a_{hp,dec,south}$ | $a_{hp,avg,south}$ | $g_{TTI,h}$ | $g_{sw,hp,s}$ |
|---|---|---|---|---|---|---|---|---|---|---|---|
| **Value** | $1.70x10^7$ | $2.00x10^7$ | $1.50x10^7$ | $6.80x10^7$ | -0.07 | -0.08 | -0.09 | -0.07 | -0.075 | 0.43 | 0.44 |

The parameters of the organic PCM are shown in Table 3.

**Table 3 PW parameters (Vadwala, 2011; DuPont, 2011).**

| Parameter | Value | Units |
|---|---|---|
| *Total heat storage capacity (Temperature range 0 to 30 °C)* | ~140 | kJ/kg |
| *Specific heat (solid phase)* | 2.384 | kJ/kg °C |
| *Thermal conductivity (solid phase)* | 0.18 | W/m K |
| *Weight* | 4.50 | kg/m$^2$ |

### *3.1.1 Passive system (heating mode)*

The EnEV 2002 commercial software program (Fachverband Transparente Wärmedämmung, 2015) has been used to simulate the TTI as a passive heating system with an integrated absorber and a thermal conductivity of 1.010 W/m K on the external wall. The results of the program are shown in Table 4.

**Table 4 Summary of parameters calculated with EnEV 2002 program for the passive heating system.**

| Parameter | Value | Units |
|---|---|---|
| $g_{h,b}$ | 0.43 | |
| $g_{n,b}$ | 0.62 | |
| $R_b$ | 3.12 | m$^2$K/W |
| $R_w$ | 0.18 | m$^2$K/W |
| $G$ | 0.44 | |
| $U_w$ | 0.3 | m$^2$K/W |
| $F_f$ | 0.86 | |
| $Fs$ | 0.9 | m$^2$ |
| $F_w$ | 1 | |
| $Fc$ | 1 | |
| $I_{s,jan,i,south}$ | 370.77 | W/m$^2$ |
| $I_{s,feb,i,south}$ | 393.52 | W/m$^2$ |
| $I_{s,mar,i,south}$ | 462.96 | W/m$^2$ |
| $I_{s,dec,i,south}$ | 347.22 | W/m$^2$ |

Therm 7.3 (LBNL, 2015) has been used to simulate the behavior of the passive heating system under the boundary conditions at night-time considering an exterior average equivalent temperature of 0°C and interior air temperature of 21°C. Apart from the heat flow direction, Fig. 4 illustrates the temperature performance of the proposed system, obtaining a temperature of 9.2°C on the outer surface of the paraffin panel.

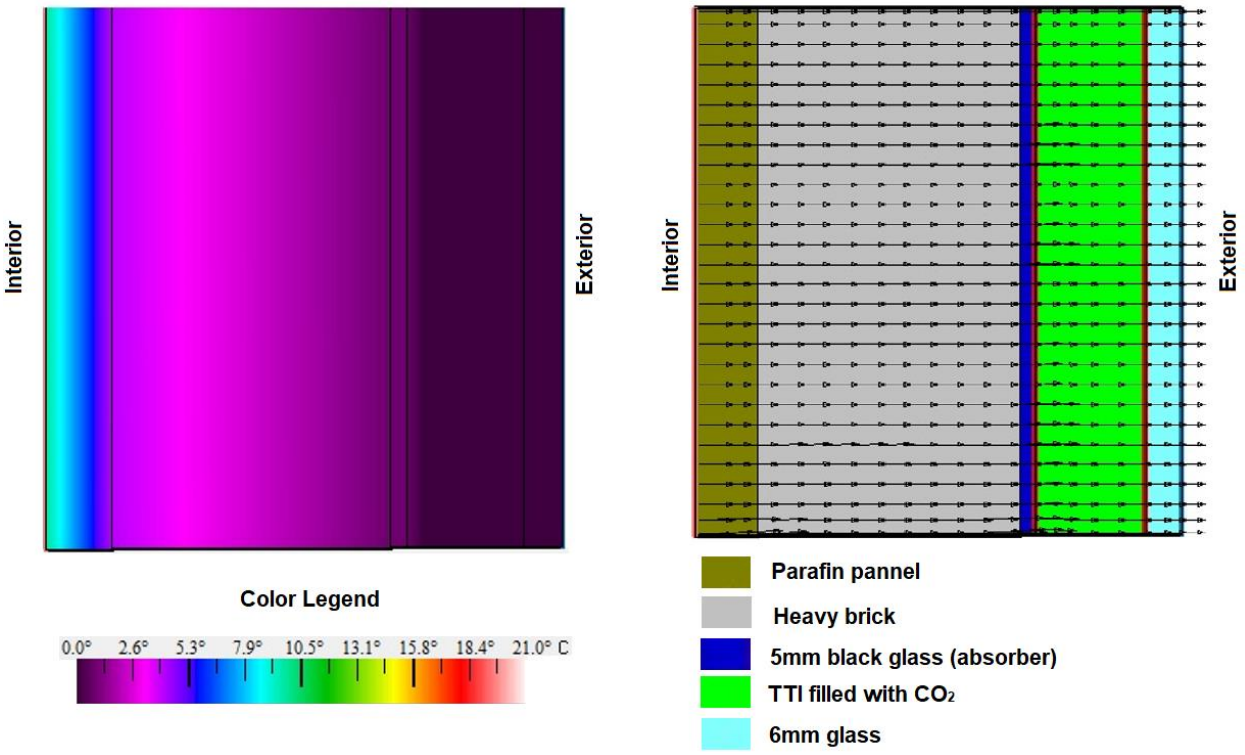


**Fig. 4. Simulation of temperature performance and heat flow direction of the passive heating system with boundary conditions at night.**

### *3.1.2 Passive system (cooling mode)*

For the cooling case, the same program has been used to simulate the behavior of the passive cooling system under the boundary conditions with an exterior average equivalent temperature of 25 °C considering a south oriented light wall and an interior temperature of 21 °C. These temperatures were assumed based on the Official Mexican Standard NOM-020-ENER-2011 (CONUEE, 2020), that suggests minimum envelope thermal properties for residential building and the study from Estrada and Almanza (2005). Also, the following solar irradiation values for Mexico City have been assumed (Estrada and Almanza, 2005):

- December: 15 MJ d $m^{-2}$
- January: 16 MJ d $m^{-2}$
- February:17 MJ d $m^{-2}$
- March: 20 MJ d $m^{-2}$

According to the simulation results shown in Fig. 5 (left), the high temperature (25 °C) occurs on the outer surface of the TTI system while the internal layer (brick) reaches a temperature of around

22.5 °C. Fig. 5 (right) also shows the heat is concentrated on the absorber. The absorber emits all radiation toward the air gap, and the $CO_2$ gas prevents the system from losing the heat toward the environment. The nano-film act a barrier against the heat, and the lines of the heat flow show the warming of the air gap.

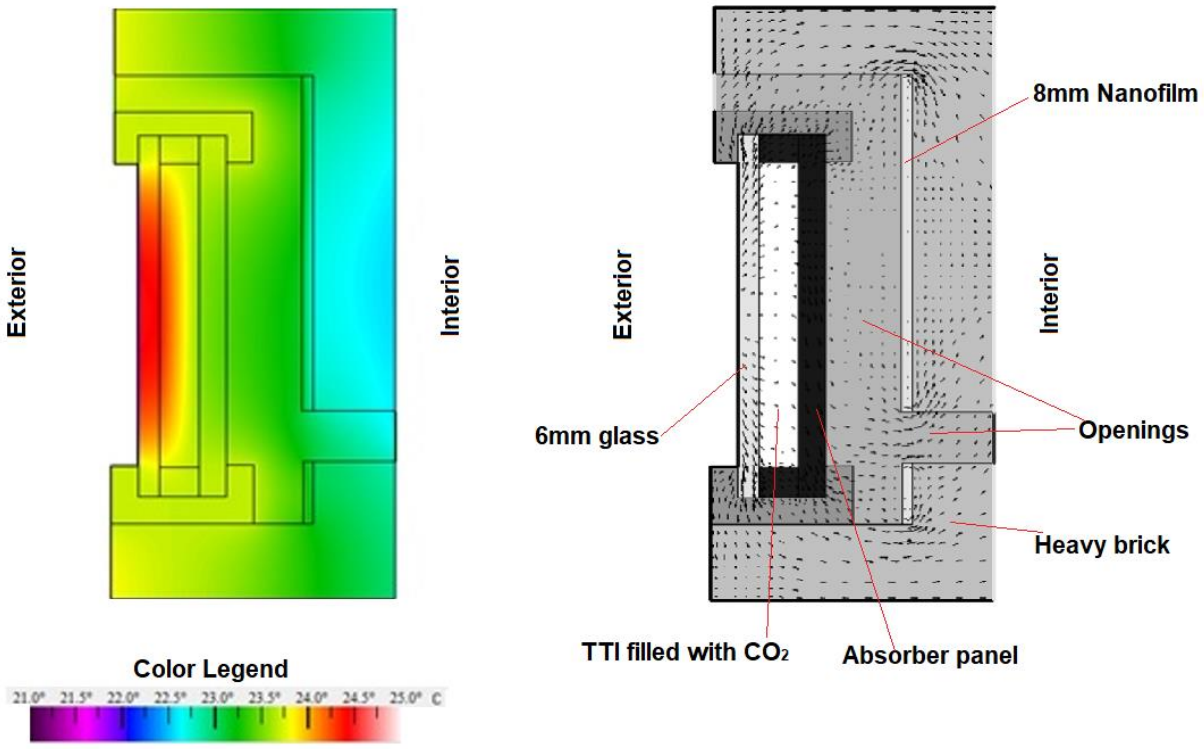


**Fig. 5. Simulation of temperature performance and heat flow direction of the passive cooling system with boundary conditions.**

To account for air velocities and to analyze the behavior of air flow into the passive cooling system, the system was modelled using Flow Design (Autodesk, 2020). For the simulation, it was assumed a wind velocity value based on real data obtained form the Mexico City's Atmospheric Monitoring Directorate (Dirección de Monitoreo Atmosférico, 2020) and gathered in December, 2019. In this period, southwest winds with velocities between 1.1-2.1 m/s were the most predominant, with a frequency of 12.3%. The CAD prototype designed and imported into Flow Design is illustrated in Fig. 6. The model has a length of 1.894 m, height of 1.178 m and a width 2.053 m. Fig. 6 shows the air behavior inside the building and the wind behavior on the exterior. According to Fig. 6 (a), the wind velocity reached a value between 0-0.69 m/s in the air discharge of TTI system (top damper). Fig. 6 (b) shows a speed of 1.357 m/s into the air duct and a pressure 0.867 Pa in stable stage. Fig. 6 (c) illustrates that the air flow covered an important interior area of room in transient stage. According to the simulations, the highest air speed reached inside the room is of 0.5 m/s. Finally, Fig. 6 (d) similarly to (b) shows the flow behavior into of air duct (floor level) when the wind flows by the low damper of the TTI system in the cooling mode.

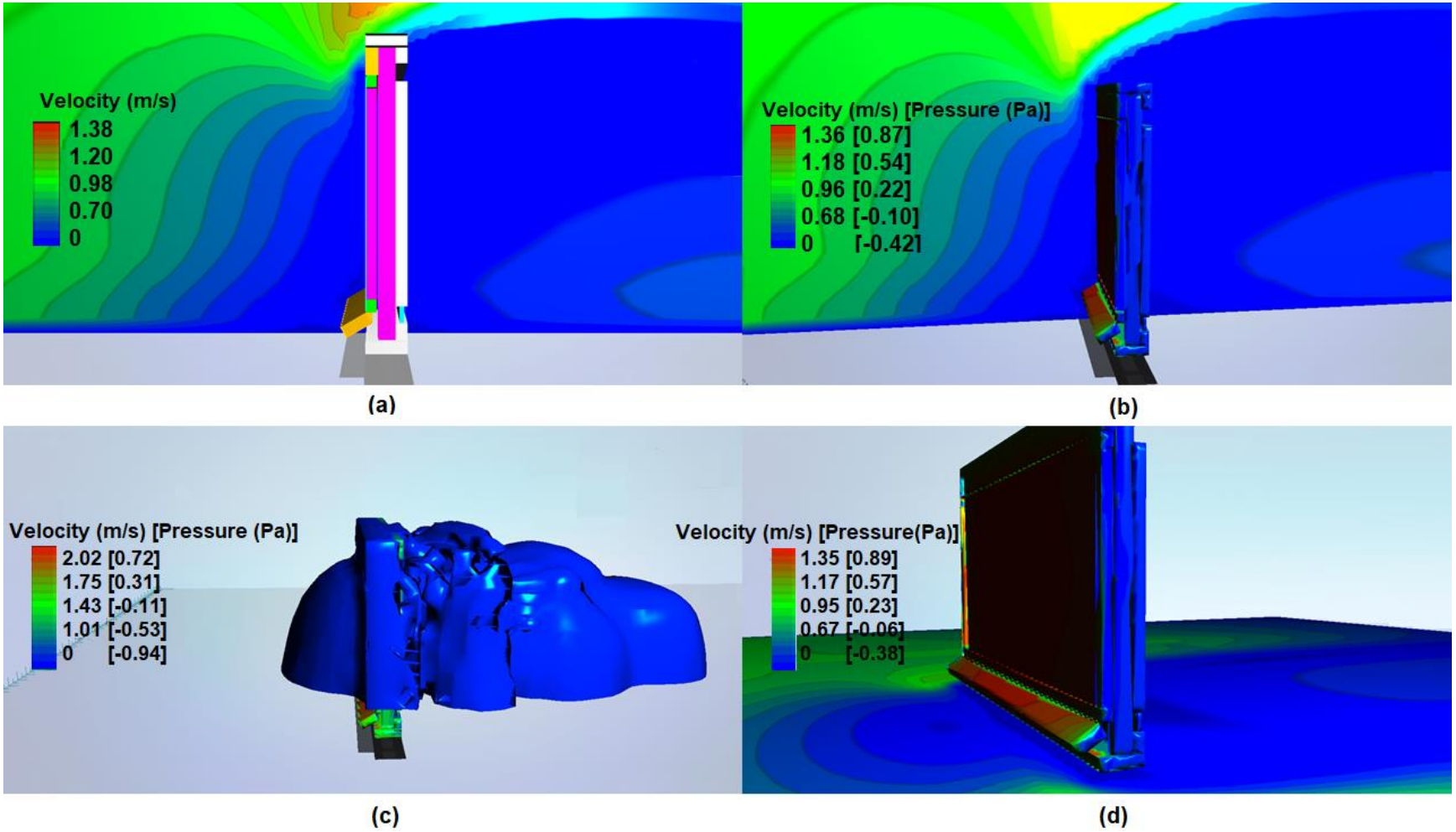


**Fig. 6. Simulations of the air speed in (a) low and top dampers, (b) low damper, (c) interior room area, and (d) low damper (floor level).**

## 4. Results and Discussions

By applying the proposed analytical model and according to eqs. (2) and (6) for $Q_{swh,hp,j}$ and $Q_{pcm}$ respectively, the heat flow rate that resulted from analyzing the TTI system and PW as passive system (heating mode) yields the values shown in Table 5. For each of the four winter months, the time of reference for calculating the heat losses in room was 43,200 seconds (12 hours).

**Table 5 Rate of heat flow of $CO_2$-filled TTI as passive heating system.**

| Parameter | Value | Units |
|---|---|---|
| $g_{TTI,n}$ | 0.62 | |
| $g_{TTI,hp,S}$ | 0.49 | |
| $R_{se}+R_b+R_s$ | 3.03 | $m^2$ K/W |
| $R_{se}+R_b+R_s+R_w+R_{si}$ | 3.33 | $m^2$ K/W |
| $(R_{se}+R_b+Rs)/(R_{se}+R_b+R_s+R_w+R_{si})$ | 0.91 | |
| $g_{swh,hp,s}$ | 0.45 | |
| $A_{swh,south}$ | 108 | $m^2$ |
| $F_f$ | 0.86 | |
| $F_s$ | 1 | |
| $F_c$ | 1 | |
| ***December*** | | |
| *Time* | 43,200 | s |
| $Q_{swh,hp,south,secember}$ | 5,091 | kJ |
| $Q_{swh,hp,south,\ december}$ | 117.84 | W |
| ***January*** | | |
| *Time* | 43,200 | s |
| $Q_{swh,hp,south,\ january}$ | 5,430 | kJ |
| $Q_{swh,hp,south,\ january}$ | 125.70 | W |
| ***February*** | | |
| *Time* | 43,200 | s |
| $Q_{swh,hp,south,\ february}$ | 5,769 | kJ |
| $Q_{swh,hp,south,\ february}$ | 133.56 | W |
| ***March*** | | |
| *Time* | 43,200 | s |
| $Q_{swh,hp,south,\ march}$ | 6,788 | kJ |
| $Q_{swh,hp,south,\ march}$ | 157.12 | W |

The $g_{swh,hp,S}$ value of 0.45 is similar to the one reported by Reim et al. (2005) in a system with two low e-coatings, an emittance of 0.08, and a combination of honey comb capillary tubes of 12 mm length with krypton gas and 16 mm with argon gas.

In the presented case study (a south façade with surface of 108 $m^2$ located on an office building in Mexico City), a heat flow of 152.12 W in March was calculated, representing the highest values among the winter season months. The rate of heat flow of the TTI system on the exterior wall is summarized in Fig. 7.

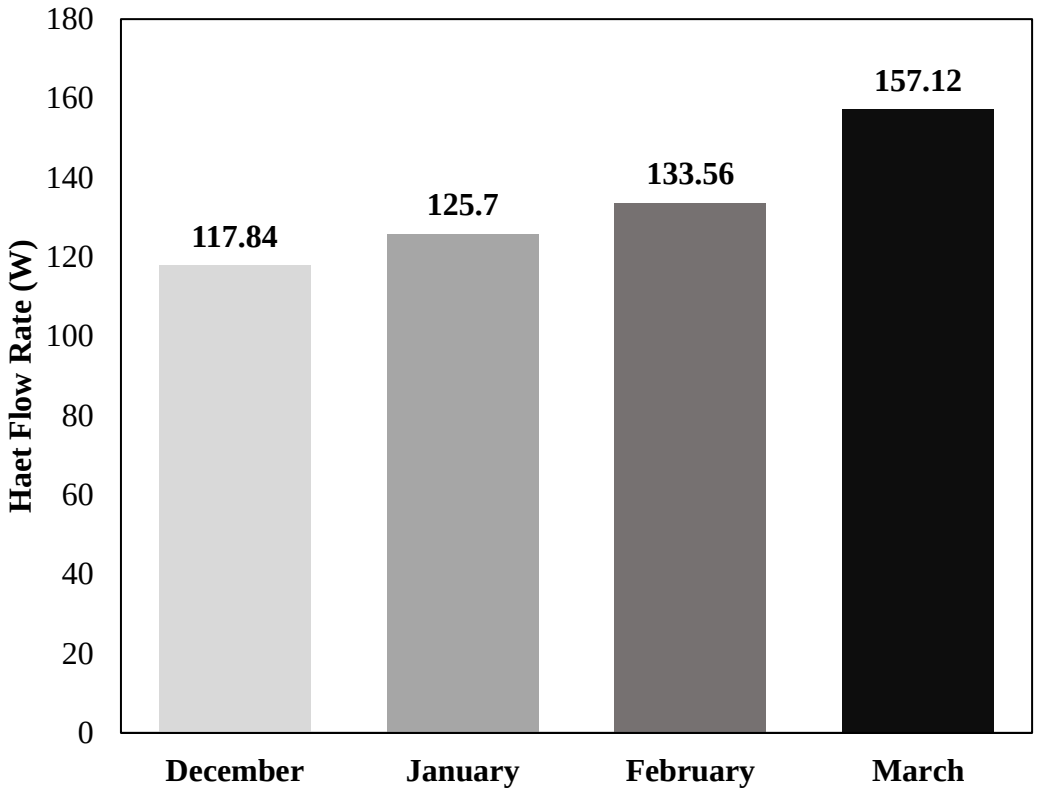


**Fig. 7. Rate of heat flow of TTI-PCM in the winter season.**

For validation purposes, Table 6 shows a comparison between the proposed model and the simulations' outputs that were presented in the previous section. The errors were found to be smaller than 0.35% between the proposed model and the more complex simulation tools.

**Table 6 Comparison between the monthly heat flow rate of the TTI-PCM system based on Eq. (4) and the program EnEV.**

| Month | $Q_{swh,hp,south,\ month}$ (W) | | |
|---|---|---|---|
| | Eq. (4) | Program EnEV | Error % |
| *December* | 117.84 | 118.25 | 0.35 |
| *January* | 125.70 | 126.13 | 0.34 |
| *February* | 133.56 | 134.02 | 0.34 |
| *March* | 157.12 | 157.67 | 0.35 |

With a heat flow rate 157.12 W for the month of March, and considering a mass of 486 g in the PW panel (rectangle enclosure with paraffin $C_{15}$-$C_{16}$ has volume 0.54 $m^3$ and 0.90 $kg/m^3$ density), heat flow per mass was found at a rate of 0.32 W/g. This heat flow per mass value is similar to the 0.35 W/g reported by Lamberg et al. (2004) and Zalba et al. (2003).

The same methodology applied to the TTI system with $CO_2$ has been applied to calculate the resulting heat flow rate on the exterior wall with other gases such as air, argon and krypton. Fig. 8 shows these results.

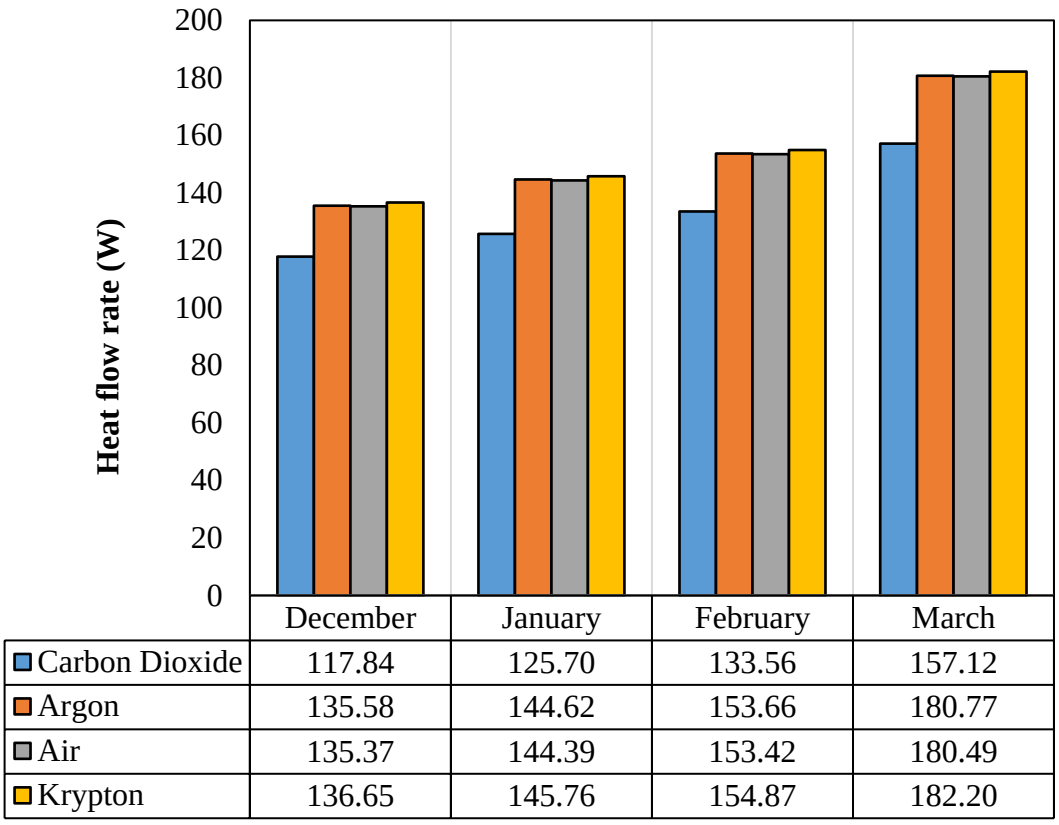


| | December | January | February | March |
|---|---|---|---|---|
| Carbon Dioxide | 117.84 | 125.70 | 133.56 | 157.12 |
| Argon | 135.58 | 144.62 | 153.66 | 180.77 |
| Air | 135.37 | 144.39 | 153.42 | 180.49 |
| Krypton | 136.65 | 145.76 | 154.87 | 182.20 |

**Fig. 8. Rate of heat flow of the TTI system with four different gases.**

As shown, the highest heat flow rate occurs in the krypton filled TTI system in March. Krypton and argon are gases with better heat gains than $CO_2$; however, their higher cost compared to air and $CO_2$ could limit its large-scale implementation.

The total heat flow in the PW ($Q_{pcm}$) is shown in Table 7.

**Table 7 Heat flow in the organic PCM.**

| Parameter | Value | Units |
|---|---|---|
| $A_{swh}$ | 108 | $m^2$ |
| $m_{PCM}$ | 486 | g |
| $\Delta T$ | 9.41 | $^oC$ |
| $Q_{pcm}$ | 78,943 | kJ |

Results suggest that PW as a passive heating system holds great potential as it can capture up to 21.9 kW. This value represents the commercial capacity of conventional furnace that uses natural gas as fuel and heating capacity of 22 kW (Rheem, 2019).

The mathematical model described in section 2.2.3 by Eq. (16) for calculating the solar transmittance, produced similar results to those obtained by Wong and Eames (2015) with the TTI-polymethyl methacrylate with a thickness of 14 mm. The solar transmittance computed by the mathematical model derived was 0.5592 with a refractive angle of $\theta_3$= 40°. Wong and Eames (2015) computed values of solar transmittance of 0.5846 and Cuce et al. (2014) of 0.97 for containers of aerogel with thickness of 1.300 nm.

This study considers a vacuum pressure of 533.4 mm Hg that is supported by a 6mm thick glass. A charge pressure of 10 bar is supported by the glass box of the TTI system. Other architectural elements such as the brick thickness of 212 mm in the exterior wall was also assumed in the simulation of the TTI system in the heating mode. The results show that the highest temperature of 25 °C is reached on the glass and the lowest temperature of 22.7 °C was computed on the wall.

Some researchers proposed the springs of Ni-Ti as actuators of air conditioners, especially for mini-split type systems; however, these smart materials have not been used as control system of air flow in passive systems. Shape memory alloy actuators can control dampers to restrict the air flow and avoid overheatingin roomsof residential buildings in spring and summer seasons. Operating temperatures of these actuators can be suggested between -10 °C and 50°C. These control systems with shape memory actuators could enable a year-round operation of the passive system to heat or cool the room when necessary .

This study has also shown that passive measures such as the TTI systems with PW board could decrease the fossil fuel energy consumption of buildings. The performance of the proposed system will depend on the building design, location, and climate conditions. It could also propose benefits such as decrease in gas bill and reduction in operation and maintenance of heating and ventilation systems. Considering the application of the system at large scale, it could act as a $CO_2$ storage system with potential reduction of the greenhouse effect.

## 5. Conclusion

This paper presented a detailed procedure to model heat gains in novel wall configurations. The proposed analytical model has been validated with simulations from commercially available tools. This theoretical model is based on refractive behavior of incident ray through the TTI and towards the absorber of cooper foil. The proposed mathematical model can be used to compute the rate of heat flow on passive heating and cooling systems.

To test the model, a passive heating/cooling system composed by an exterior wall integrated with a $CO_2$-filled TTI and an organic phase change material (PCM) has been used. The proposed wall design has the intention to maximize heat capture from solar radiation during the winter season; where the organic PCM is used to deliver heat in the interior while the $CO_2$-filled TTI is integrated to release heat to the exterior. A $CO_2$-filled TTI and organic PCM could complement each other as passive systems of heating and cooling in buildings. This is mainly due to the TTI's reductions

in heat losses that contributes to lower heat demand in the winter season. Thermal conductivity is an important factor to consider in the evaluation of performance of the TTI system. Outputs suggest that factors such as $g_{TTI,h}$, $g_{TTI}$, and $Z_{So}$ need to be further investigated.

The comparative study has shown that a gas with low thermal conductivity acts as a large thermal barrier that avoids heat flow toward the environment. Thus, gases such as krypton and xenon could be used with the TTI system as they have a lower thermal conductivity than $CO_2$.

For future research the following work is expected to be carried out:

- Replacement of the nano-film by vacuum insulation.
- Alloy of Ni-Ti based on two-way effect could be integrated into the passive cooling system. Also, a damper at the bottom of the wall could be coupled with shape memory actuators.
- Analysis of waste heat flow recovery of the TTI system will be performed, as this could further reduce building energy demand.
- Use refrigerants such as 134 A in TTI due to low thermal conductivity.

## Acknowledgements

The authors express their gratitude to Dr. Mark Miller and Dr. Sandra Vaiciulyte for their collaboration as English reviewers of this manuscript. The corresponding author acknowledges the support from ‘Coordinación de la Investigación Científica’ from the ‘Universidad Nacional Autónoma de México’ through a scholarship to pursue posdoctoral studies with a grant number: CJIC/CTIC/1011/2019

## References

Athienitis AK., Ramadan H., 2000. Numerical model of a building with transparent insulation. Solar Energy. 67(1-3), 101-9.

Autodesk. 2020. Flow Design. Available from: https://www.autodesk.com/products/flow-design/overview

Bendong, Y., Qinyang, J., Wei, H., Zhonting. H., Hongbing, C., Jie, J., Gang, X., 2018. The performance analysis of a novel TC-Trombe wall system in heating seasons. Energy Conversion and Management. 164, 242-261.

Berge, A., Johansson, P., 2012. Literature Review of High Performance Thermal Insulation. Report in Building Physics. Sweden: Chalmers University of Technology.

Briga Sá, A., Boaventura-Cunha, J., Lanzinha, J.C., and Paiva, A., 2017. An experimental analysis of the Trombe wall temperature fluctuations for high range climate conditions: Influence of ventilation openings and shading devices. Energy and Buildings.138, 546-558.

Buratti C., Moretti E., 2011. Transparent insulating materials for buildings energy saving: experimental results and performance evaluation. Third International Conference on Applied Energy. 1421-32.

Cengel Y., 2004. Heat transfer: a practical approach, 2nd. Ed. Mc Graw Hill, New York.

Chel, A., Kaushik, G., 2018. Renewable energy technologies for sustainable development of energy efficient building. Alexandria Engineering Journal. 57, 655-669.

CONUEE, 2020. Norma Oficial Mexicana NOM-020-ENER-2011, Eficiencia energética en edificaciones - Envolvente de edificios para uso habitacional. [*Trans. Official Mexican Standard NOM-020-ENER-2011, Energy efficiency in buildings.- Envelope for residential buildings*]. Comisión Nacional para el Uso Eficiente de la Energía Available from: https://www.gob.mx/cms/uploads/attachment/file/181660/NOM_020_ENER_2011.pdf

Cuce E., Cuce PM., Wood CJ., Riffat SB., 2014. Toward aerogel based thermal superinsulation in buildings: 731 A comprehensive review. Renewable Sustainable Energy Reviews. 34, 273-299.

Cuce E., Riffat SB., 2015. A state of the art review on innovative glazing technologies. Renewable Sustainable Energy Reviews. 41, 695-714.

Dirección de Monitoreo Atmosférico, 2020. Estadísticas, gráficos interactivos (Trans: Atmospheric Monitoring Directorate, Statistics, interactive charts) Available from: http://www.aire.cdmx.gob.mx/default.php?opc=%27aqBhnmQ=%27

DuPont, 2011. Energain, energy-saving thermal mass systems. Luxembourg: DuPont de Nemours.

Estrada V., Almanza R., 2005. Irradiaciones global, directa y difusa, en superficies horizontales e inclinadas, así como irradiación directa normal, en la República Mexicana (*Trans: Global, direct and diffuse irradiations and normal direct irradiation on horizontal and inclined surfaces in Mexico*). Distrito Federal: Instituto de ingeniería, Universidad Nacional Autónoma de México.

Fachverband Transparente Wärmedämmung (*Trans: Professional Association for Transparent Insulation*), 2015. EnEV 2002 Transparente Wärmedämmung, http://umwelt-wand.de/ti/architect/tools.html. [accessed 26.04.15]

Ji, J., Lou C. L., Sun, W., Yu, H. C., He, W., Pei, G. 2009. An improved approach for the application of Trombe wall system to building construction with selective thermo-insulation facades. Chinese Science Bulletin. 54, 1949-1956.

Hauser R, Geibler S, Platzer WJ., 1996. Ecological and energetic evaluation of transparent insulation systems. Proc. EuroSun. 74-9.

Hernández, V., Morillón, D., Fernández, J., Best, R., Almanza, R, and Chargoy, N., 2006. Experimental and numerical model of wall like solar heat discharge passive system. Applied Thermal Engineering. 26, 2464-2469.

Hernández, V.H., Morillón, D., Fernández, J.L., 2010. Design recommendations for heat discharge systems in walls. Applied Thermal Engineering. 30,1616-1620.

Hernández, V.H., Morillón, D., 2013. Analytical model for double skin roofs. Applied Thermal Engineering. 60, 218-224.

Huenchuñir M., 2002. Sistemas de Fachada con Aislación Térmica Transparente (*Trans: Facade Systems with Transparent Thermal Insulation*). Revista BIT. 25, 54-56.

Kaushika, N.D. and Arulanantham M., 1995. Radiative heat transfer across transparent honeycomb insulation materials. Journal Communications in Heat and Mass Transfer. 22(5), 751-760.

Kaushika, N.D. and Sumathy, K., 2003. Solar transparent insulation materials: a review. Renewable and Sustainable Energy Reviews. 7, 317-351.

Konstantinidou C., 2010. Integration of thermal energy storage in buildings (Master Thesis). Texas, USA: Department of Architecture, University of Texas, Texas.

Kundakci Koyunbaba, B. and Yilmaz, Z., 2012. The comparison of Trombe wall systems with single glass, double glass and PV panels. Renewable Energy. 45, 111-118.

Lamberg P., Lehtiniemi R., Hennell AM., 2004. Numerical and experimental investigation of melting and freezing processes in phase change material storage. International Journal of Thermal Sciences. 43, 277-287.

LBNL (Lawrence Berkeley National Laboratory), 2015. Therm 7.3 software for analyzing optical properties of glazing systems, (http://windows.lbl.gov/software/therm/therm.html) [accessed 26.04.15].

Lokesh J., Sharma S., 2009. Phase change materials for day lighting and glazed insulation in buildings. Journal of Engineering Science and Technology. 4(3), 323-27.

Mohd Isa M., Zhao X., Yoshino H., 2010. Preliminary study of passive cooling strategy using a combination of PCM and copper foam to increase thermal heat storage in building façade. Sustainability. 2(8), 2365-81.

Ochs M., Haller A., Simmler H., 2000. A simple method to calculate the heat gains of solar wall heating with transparent insulation. Third ISES Europe Solar Congress EuroSun. 19-22.

Olgyay, V., 1963. Design with Climate: Bioclimatic Approach to Architectural Regionalism. Princeton University Press. Princeton, New Jersey.

Paneri, A., Wong,L., Burek, S. 2019. Transparent insulation materials: An overview on past, present and future developments. Solar Energy. 184, 59-83.

Parker, J., Brown, R., 2013. Application note sustainable heating and cooling. No Cu0155, Brussels, Belgium; European Copper Institute.

Platzer, WJ., 1997. Advances in transparent insulation technology. Proc. of the Int. Conf. on Build. Envelope systems and technologies. 349-54.

Pérez, J-B., Cabanillas, R-E., Hinojosa,J-F., Borbón, A-C. 2011. Estudio numérico de la Resistencia térmica en muros de bloques de concreto hueco con aislamiento térmico (*Trans: Numerical study of thermal resistance in hollow concrete block walls with thermal insulation*). Información tecnológica. 22(3), 27-38.

Platzer, WJ., 1999. Energetische Bewertung von Transparenter Wärmedämmung (*Trans: Energetic evaluation of transparent thermal insulation*). Bauphysik. 21(2), 64-76.

Reim M., Körner W., Manara J., Korder S., Arduini-Shuster M., Ebert H-P, Fricke J., 2005. Silica aerogel granulate material for thermal insulation and daylighting. Solar Energy. 79(2), 131-9.

Rheem, 2019. Rheem Prestige Series EcoNet Enabled Modulating Upflow Gas Furnaces R98V-Series, 2019. Available from: https://cdn.globalimageserver.com/FetchDocument.aspx?ID=21864A82-141E-4D13-AC61-32A32C211695

SENER/CONUEE, 2001. Norma Oficial Mexicana NOM- ENER-008-2001, Eficiencia energética en edificaciones, envolvente de edificios no residenciales (*Trans: Official Mexican Standard NOM- ENER-008-2001, Energy efficiency in buildings, envelope of non-residential buildings*), CDMX, Mexico.

Swirska-Perkoswka, J., Kucharczyk, A., Wyrwal, J. 2020. Energy efficiency of a solar wall with transparent insulation in polish climatic conditions. Energies. 13, 859. 1-21.

Szokolay, S.V., 2004. Introduction to architectural science the basis of sustainable design (1st. Ed.). Oxford, United Kingdom: ELSEVIER/Architectural Press.

Thirugnanam C., Marimuthu, P., 2013. Experimental analysis of latent heat thermal energy storage using paraffin wax as phase change material. Journal International of Engineering and Innovative Technology. 3(2), 372-376.

Vadwala P., 2011.Thermal Energy Storage in Copper Foams filled with Paraffin Wax (Master Thesis). Toronto, Canada: Department of Mechanical and Industrial Engineering, University of Toronto.

Veinberg BP., Veinberg VB., 1959. Optics in equipment for the utilization of solar energy. Moscow: State Publishing House of Defense Industry.

Wallner GM., Hausner R., Hegedys H., Shombermayr H., Lang RW., 2006. Application demonstration and performance of a cellulose triacetate polymer film based transparent insulation wall heating system. Sol. Energy. 80(11), 1410-1416.

Wasser Resources. 2020. Solar window coating e time energy. Available from: https://wasserresources.com/power-conservation/etime-heatshield/

Wong IL., Eames PC., 2015. A method for calculating the solar transmittance, absorptance and reflectance of a transparent insulation system. Solar Energy. 111, 418-25.

Wong IL., Eames PC., Perera RS., 2007. A review of transparent insulation systems and the evaluation of payback period for building applications. Solar Energy. 81(9), 1058-1071.

Yeang, K., 2001. El rascacielos ecológico (*Trans: The ecological skyscraper*), 1st. Ed. Barcelona, España: Editorial Gustavo Gili, SA.

Zalba B., Marín J M., Cabeza L F., Mehling H., 2003. Review on thermal energy storage with phase change: materials, heat transfer analysis and applications. Applied Thermal Engineering. 23, 251-83.